Journal of Experimental Botany, Vol. 68, No. 13 pp. 3427–3440, 2017
doi:10.1093/jxb/erx192 Advance Access publication 13 June 2017

RESEARCH PAPER

The asparagine-rich protein NRP interacts with the *Verticillium* effector PevD1 and regulates the subcellular localization of cryptochrome 2

Ruimin Zhou[1,†], Tong Zhu[1,†], Lei Han[2], Mengjie Liu[2], Mengyuan Xu[1], Yanli Liu[1], Dandan Han[1], Dewen Qiu[2,*], Qingqiu Gong[3,*] and Xinqi Liu[1,*]

[1] State Key Laboratory of Medicinal Chemical Biology, Department of Biochemistry and Molecular Biology, College of Life Sciences, Nankai University, Tianjin 300071, China
[2] State Key Laboratory for Biology of Plant Diseases and Insect Pests, Chinese Academy of Agricultural Sciences, Institute of Plant Protection, Beijing 100081, China
[3] Tianjin Key Laboratory of Protein Science, Department of Plant Biology and Ecology, College of Life Sciences, Nankai University, Tianjin 300071, China

* Correspondence: dewenqiu@hotmail.com; gongq@nankai.edu.cn; liu2008@nankai.edu.cn
† Co-first authors.

Received 27 January 2016; Editorial decision 15 May 2017; Accepted 16 May 2017

Editor: Katherine Denby, York University

Abstract

The soil-borne fungal pathogen *Verticillium dahliae* infects a wide range of dicotyledonous plants including cotton, tobacco, and Arabidopsis. Among the effector proteins secreted by *V. dahliae*, the 16 kDa PevD1 induces a hypersensitive response in tobacco. Here we report the high-resolution structure of PevD1 with folds resembling a C2 domain-like structure with a calcium ion bound to the C-terminal acidic pocket. A yeast two-hybrid screen, designed to probe for molecular functions of PevD1, identified Arabidopsis asparagine-rich protein (NRP) as the interacting partner of PevD1. Extending the pathway of *V. dahliae* effects, which include induction of early flowering in cotton and Arabidopsis, NRP was found to interact with cryptochrome 2 (CRY2), leading to increased cytoplasmic accumulation of CRY2 in a blue light-independent manner. Further physiological and genetic evidence suggests that PevD1 indirectly activates CRY2 by antagonizing NRP functions. The promotion of CRY2-mediated flowering by a fungal effector outlines a novel pathway by which an external stimulus is recognized and transferred in changing a developmental program.

Key words: CRY2, flowering time, fungal infection, localization, NRP, PevD1.

Introduction

Field plants are constantly challenged by a combination of abiotic and biotic stresses (Kissoudis *et al.*, 2014). In order to survive and reproduce, plants have to evaluate the stress conditions in a timely manner and respond appropriately (Hirayama and Shinozaki, 2010; Kissoudis *et al.*, 2014). In the case of biotrophic pathogen invasion, localized cell death, termed the hypersensitive response (HR), is promptly induced at the infection site to restrict nutrient loss and the spread of pathogens (Spoel and Dong, 2008). Meanwhile, systemic acquired resistance (SAR) is elicited at the infected

tissues, which then spreads to the rest of the plant and is long-lasting (Kachroo and Robin, 2013). Apart from the defense reactions, stressed plants may change their developmental programs, such as flowering time. For example, tomato plants infected with phytoplasma fail to complete their floral transition (Wei *et al.*, 2013). In contrast most Arabidopsis accessions infected with the fungal vascular pathogen *Verticillium dahliae* flower earlier (Veronese *et al.*, 2003). Arabidopsis plants treated with the bacterial pathogen *Pseudomonas syringae* elicitor, flg22, also shorten their clock period (Zhang *et al.*, 2013*b*).

Recent studies have established several critical links between light, circadian clock, and pathogenesis-related (PR) gene-mediated resistance to various pathogens (Roden and Ingle, 2009). The red/far-red-light photoreceptors phytochromes A and B are required for salicylic acid-induced PR gene expression (Genoud *et al.*, 2002) and induction of SAR (Griebel and Zeier, 2008). The blue-light photoreceptors cryptochrome 2 (CRY2) and phototropin 2 have both been found to be required for preventing the turnover of the resistance (R) protein HRT (Jeong *et al.*, 2010). Cryptochrome 1 (CRY1) positively regulates R protein-mediated immune response against *P. syringae* by inducing PR gene expression (Wu and Yang, 2010). Mis-expression of clock genes such as circadian clock-associated 1 (CCA1), late and elongated hypocotyl (LHY) compromises basal and *R*-gene-mediated resistance to *P. syringae* and/or the oomycete pathogen *Hyaloperonospora arabidopsidis* (Wang *et al.*, 2011; Zhang *et al.*, 2013*b*). Nevertheless, only a few protein–protein interaction-based signaling pathways that link effector proteins to clock components have been established.

The soil-borne fungal pathogen *V. dahliae* can infect over 200 dicotyledonous plant species and induce vascular wilting disease that leads to yield loss worldwide (Miao *et al.*, 2010). Germination of conidia can be observed within hours after inoculating Arabidopsis roots with *V. dahliae*, and the resulting hyphae penetrate into the roots within 48 h post-inoculation (Zhao *et al.*, 2014). Within 5 d a hyphal net can be observed in the xylem of the root (Zhao *et al.*, 2014). During the process *V. dahliae* secrets hundreds of proteins, of which dozens have been shown to be involved in pathogen–host interaction (Campbell, 1989). Unfortunately, apart from a group of cellulose degrading enzymes (St Leger *et al.*, 1997), pathological functions of most effectors remain unknown. Of the known *V. dahliae* effectors, Ave1 was identified as acting through the Ve1 receptor in both Arabidopsis and tomato. Ave1 activates immune response in plants containing the *Ve1* gene, which are resistant to wilting. In contrast, Ave1 enhances virulence in *Ve1*-null plants that are susceptible to *V. dahliae* (de Jonge *et al.*, 2012). Another *V. dahliae* effector, VdIsc1, can suppress salicylate-mediated innate immunity in plants by acting as an isochorismatase (Liu *et al.*, 2014).

We recently identified a new *V. dahliae* effector, PevD1 (Han *et al.*, 2012). It elicits HR in tobacco (Wang *et al.*, 2012) and induces SAR to tobacco mosaic virus (Wang *et al.*, 2012). Nonetheless, the underlying molecular mechanism remains to be discovered.

To elucidate the biochemical and genetic basis of PevD1-induced pathological and physiological changes *in planta*, we searched for PevD1 interacting partners by yeast two-hybrid (Y2H) screens. The asparagine-rich protein (NRP) was identified as a PevD1-interacting protein in Arabidopsis, and a consecutive Y2H identified CRY2 as an NRP-interacting component.

NRP was originally found to be activated as a component of the early pathogen response in soybean (Ludwig and Tenhaken, 2001; Hoepflinger *et al.*, 2011). Expression of the protein is also induced by endoplasmic reticulum stress in soybean (Costa *et al.*, 2008; Hoepflinger *et al.*, 2011). Further study in Arabidopsis revealed that NRP is unregulated in response to various stress conditions (Hoepflinger *et al.*, 2011). NRP is composed of two domains. The N terminus is rich in asparagine, and the C terminus contains a development and cell death (DCD) domain, which is highly conserved throughout the plant kingdom and postulated to be involved in cell death (Tenhaken *et al.*, 2005). Recently, NRP was shown to serve as a signaling center in endoplasmic reticulum stress, osmotic stress, drought, and leaf senescence, and the NRP-mediated cell death signaling pathway is likely conserved in the plant kingdom (Reis *et al.*, 2016).

Numerous studies have revealed versatile functions of cryptochromes, including CRY2, in mediating the circadian rhythm, stomata opening, guard cell development, stress response, cell cycle, programmed cell death, fruit and ovule development, and seed dormancy (Yu *et al.*, 2010). CRY2 senses blue light and predominantly regulates photoperiod-induced flowering. CRY2 transgenic plants flower early in short days and *cry2* mutants flower late in long days (Guo *et al.*, 1998). By regulating the activation of downstream flowering genes, such as *CONSTANS* (*CO*), *FLOWERING LOCUS T* (*FT*), and *SUPPRESSION OF OVEREXPRESSION OF CO 1* (*SOC1*) (Yoo *et al.*, 2005), CRY2 has an essential role in flowering time control of Arabidopsis. In recent years, two mechanisms underlying CRY2-mediated floral transition have been revealed. One is that CRY2 interacts with the COP1-interacting protein SUPPRESSOR OF PHYTOCHROME A 1 (SPA1) in a blue light-dependent manner, and SPA1 acts genetically downstream of CRY2 to regulate blue light suppression of the COP1-dependent degradation of CO (Zuo *et al.*, 2011). The other mechanism involves the blue light-dependent physical interaction of CRY2 with the CRY POCHROME-INTERACTING BASIC-HELIX-LOOP-HELIX (CIB) transcription factors that directly activate *FT* transcription (Liu *et al.*, 2008; Liu *et al.*, 2013; Liu *et al.*, 2016). As the central regulator of flowering, CRY2 is also involved in the process of pathogen infection. For example, CRY2 is required for preventing the turn-over of the R protein HRT (Jeong *et al.*, 2010).

So far, CRY2 has been considered to exclusively function in the nucleus, where it can be phosphorylated for activation in a blue light-dependent manner, and then ubiquitinated and degraded (Guo *et al.*, 1999; Kleiner *et al.*, 1999; Yu *et al.*, 2007; Zuo *et al.*, 2012). In this report, we found that NRP could tether CRY2 in the cytoplasm and change its function, demonstrating that CRY2 might be localized outside

the nucleus under certain conditions. We also suggest that a PevD1–NRP–CRY2 pathway may be responsible for the early flowering phenotypes observed in cotton and Arabidopsis following *V. dahliae* infection.

Methods

Protein expression, crystallization, and structural determination of PevD1

Protein expression, purification, crystallization, data collection and structural determination were performed as described previously (Han *et al.*, 2012). PHENIX was used for refinement, and a calcium ion was determined based on electron density and surrounding environment. The results of data collection and structural determination are summarized in Supplementary Table S1 at *JXB* online.

Immunostaining of PevD1

Roots of seedlings infected with *V. dahliae* for a week were used to perform the immunostaining assay, according to the method described previously (Friml *et al.*, 2003). The anti-PevD1 antibody was generated by immunizing rabbits with purified PevD1 and was purified by Protein A resin. The specificity of the antibody was detected and confirmed to be suitable for experimental use. The second antibody, goat anti-rabbit IgG (H+L) conjugated with Rhodamine Red-X, was purchased from Jackson ImmunoResearch Laboratories.

Yeast two-hybrid assay

Yeast two-hybrid (Y2H) experiments were performed with the Matchmaker™ Gold Yeast Two-Hybrid System as described by the manufacturer (Clontech). Matchmaker™ Pre-transformed library-Universal Arabidopsis was purchased from Clontech. PevD1 and NRP were used as bait proteins independently.

Bimolecular fluorescence complementation

The *NRP* gene was cloned into the pSPYNE173 vector, and *PevD1* and *CRY2* genes were cloned into pSPYCE (M) vector. As a result, NRP was fused to the N-terminal part of yellow fluorescent protein (YFP; NRP-YN), and PevD1 and CRY2 were fused to the C-terminal part of YFP (PevD1-YC, CRY2-YC). These constructs were then introduced into *Agrobacterium tumefaciens* strain GV3101. Five-week-old tobacco (*Nicotiana benthamiana*) plants were inoculated on leaves with transformed Agrobacterium according to protocols described previously (Schütze *et al.*, 2009). Fluorescence generated by protein interaction was visualized under a Leica TCS SP8 confocal microscope at a wavelength of 550 nm.

In vitro *pull-down assay*

6×His tagged PevD1 and glutathione *S*-transferase (GST)-fused DCD domain of NRP expressed and purified from *E. coli* were used for a GST pull-down assay, and retaining bands on glutathione (GTH)-Sepharose were detected by both anti-6×His antibody and anti-GST antibody. To check the interaction of NRP and CRY2, the GST-fused DCD domain of NRP was used to carry out a GST pull-down assay against green fluorescent protein (GFP)-fused CRY2, which was extracted from *GFP-CRY2* transgenic plants (Wang *et al.*, 2006), and the retaining bands on GTH-Sepharose were detected by both anti-GFP antibody and anti-GST antibody.

Plant growth condition and generation of transgenic plants

The mutants and transgenic lines of NRP (*NRP-GFP*, *nrp*) and CRY2 (*GFP-CRY2*, *cry2*) were generous gifts of Drs Raimund Tenhaken (University of Salzburg, Austria) and Hongtao Liu (Institute of Plant Physiology and Ecology, Chinese Academy of Sciences). The *PevD1-RFP* and *NRP-RFP* fused genes were cloned into pCAMBIA1302 vector, *PevD1-RFP* was introduced into the *Arabidopsis thaliana* ecotype Columbia (Col) or *cry2* mutant, and *NRP-RFP* was introduced into the *GFP-CRY2* transgenic lines (in Col background) by the floral dip transformation method (Zhang *et al.*, 2006). The seeds were harvested, surface sterilized in 75% ethanol solution, kept at 4 °C for 3 d for vernalization, then screened using 25 mg l^{-1} hygromycin or 0.1% glufosinate (Basta). To observe the phenotypes, the seeds were sown into compound soil directly. About nine plants were grown per cup under cool white fluorescent lights with an approximate irradiance of 110 μmol m^{-2} s^{-1} for a 16-h day and 8-h night period. Temperature was maintained at 22 °C. For blue light stimulation, the plants were exposed under blue light diodes with an approximate irradiance of 5 μmol m^{-2} s^{-1} at λ_{max} 469 nm for 20 min before digestion.

Immunoprecipitation assay by GFP-Trap

Four-week-old plants were harvested and homogenized in 10 ml of protein extraction buffer (10 mM $MgCl_2$, 150 mM NaCl, 50 mM Tris–HCl pH7.5, 1 mM phenylmethylsulfonyl fluoride, 0.5% Triton X-100, 2% β-mercaptoethanol) with a mortar. The homogenate was centrifuged at 13 800 *g* for 15 min. The supernatant was concentrated into 500 μl and mixed with GFP-Trap beads (GFP-Trap®_A, Chromotek) for 40 min. The beads were collected by centrifugation at 5000 *g* for 2 min, and then washed twice with washing buffer (10 mM Tris–HCl pH7.5, 150 mM NaCl, 0.5 mM EDTA). The GFP-Trap beads were resuspended in 100 μl PBS, and prepared with SDS loading buffer for western blot.

Arabidopsis root inoculation with V. dahliae

Seven-day-old Arabidopsis (Col-0) seedlings grown on 1/2 MS medium in Petri dishes were inoculated with 2 μl drop of conidial suspension (2×10^5 conidia ml^{-1}), then transplanted into soil 3 d later. Uninfected controls were treated with a 2 μl drop of water at the same time. The culture and phenotype observation that followed were the same as above. Hyphae of *V. dahliae* were grown on potato dextrose agar. Conidia were harvested 5 d later by flooding the surface of plates with sterile distilled water, and then filtered through two layers of sterile cheesecloth (Veronese *et al.*, 2003).

Localization of CRY2 and colocalization of NRP and CRY2

For localization observation of CRY2, the *GFP-CRY2* or *NRP-RFP GFP-CRY2* transgenic plants were grown. Fluorescence was visualized under a Leica TCS SP8 confocal microscope at wavelengths of 488 nm and 561mm for GFP and red fluorescent protein (RFP), respectively. For colocalization observation on *N. benthamiana*, *CRY2* was cloned into pCAMBIA1302 to generate *35S:GFP-CRY2*. *NRP* was cloned into a modified pCAMBIA1302 vector with RFP replacing GFP to generate *35S:NRP-RFP*. The constructs were transformed into *Agrobacterium tumefaciens* strain GV3101. After the inoculation of agrobacteria on 5-week-old *N. benthamiana* leaves, fluorescence was visualized as above (Schütze *et al.*, 2009).

Fractionation of plant cells

Four-week-old Arabidopsis rosette leaves were cut into 1 mm pieces. All samples were soaked in a digestion system (1.5% Driselase, 0.4 M mannitol, 20 mM KCl, 10 mM $CaCl_2$, 0.1% BSA, 5 mM β-mercaptoethanol, 20 mM MES, pH 5.7) for 4 h at room temperature. The whole system were diluted by cold equal volume of W5 buffer (154 mM NaCl, 125 mM $CaCl_2$, 5 mM KCl, 5 mM glucose, 2 mM MES, pH 5.8), and were filtered through three layers of gauzes to collect protoplasts. The collected protoplasts were resuspended in 10% W5 buffer and vortexed for 1 min. The cytoplasm and nucleus

were then separated by centrifugation at 300 *g* for 5 min. CRY2 was detected by a polyclonal antibody from Santa Cruz Biotechnology.

FM4-64 staining

Seven-day-old seedlings (infected or uninfected) were immersed in 17 μM FM4-64 solution for 3 min on ice in the dark. Subsequent to an extensive wash in water four times, the seedlings were incubated in 1/2 MS liquid culture and collected at 10 or 40 min. The roots of seedlings were then observed under a Leica TCS SP8 confocal microscope at a wavelength of 515 nm.

RNA extraction, RT-PCR, and quantitative RT-PCR analysis

Small scale RNA extractions were performed with TRIzol reagent (Invitrogen) following the manufacturer's instructions. Reverse transcription (RT) and first strand cDNA synthesis were carried out using TransScript First-Strand cDNA Synthesis SuperMix (Transgene). Quantitative RT-PCR was carried out using standard procedure as described (Pfaffl, 2001) and UBQ10 expression levels were used as internal controls for normalization. Forty amplification cycles including 95 °C for 15 s, 60 °C for 10 s, and 72 °C for 60 s were used. Cycle threshold values were calculated by Realplex 2.2. The primers used in these experiments are summarized in Supplementary Table S2.

Results

Crystal structure of PevD1 reveals a C2 domain-like folding

To gain structural insights into the molecular functions of PevD1, the protein was crystallized. The crystal structure of PevD1 up to 1.85 Å resolution revealed a 10-β-strand β-barrel (Fig. 1A), reminiscent of a C2 domain or lectin fold. A DALI search based on similarity of three-dimensional structure revealed that PevD1 has considerable similarities to the C2 domains of synaptotagmin and phosphatidylinositol-4,5-bisphosphate 3-kinase with a *Z*-score of 4.2 (PDB code 1W16 and 3PS6, respectively) (Fig. 1B, C). The C2 domain is involved in targeting proteins to membranes, and its lipid-binding property is often mediated by coordinated calcium ions (Corbalan-Garcia and Gómez-Fernández, 2014). Indeed, a calcium atom was identified in an acidic patch on the surface of PevD1 (Fig. 1D), which is coordinated by the carbonyl oxygen of Tyr116, Leu148, OD1 in the side-chain of Asp146, and a chloride ion (Fig. 1E), reminiscent of calcium coordination in the canonical C2 domain. Further, the atomic absorption spectrum confirmed the presence of calcium in the protein. Interestingly, the β-barrel core of PevD1 has a similar fold to a previously reported structure of an ethylene-inducing peptide 1 (Nep1)-like protein (NLP), an elicitor protein isolated from the phytopathogenic oomycete *Pythium aphanidermatum* (Ottmann *et al.*, 2009*a*), despite PevD1 being much shorter (~155 residues) than NLPs (~230–260 residues) (Fig. 1F).

The interaction of PevD1–NRP and NRP–CRY2

To study the pathological roles of PevD1, a yeast two-hybrid (Y2H) screen was carried out. NRP (At5g42050) was identified repeatedly as PevD1-interacting. Then, in a consecutive screen for NRP-interacting partners, CRY2 was recovered

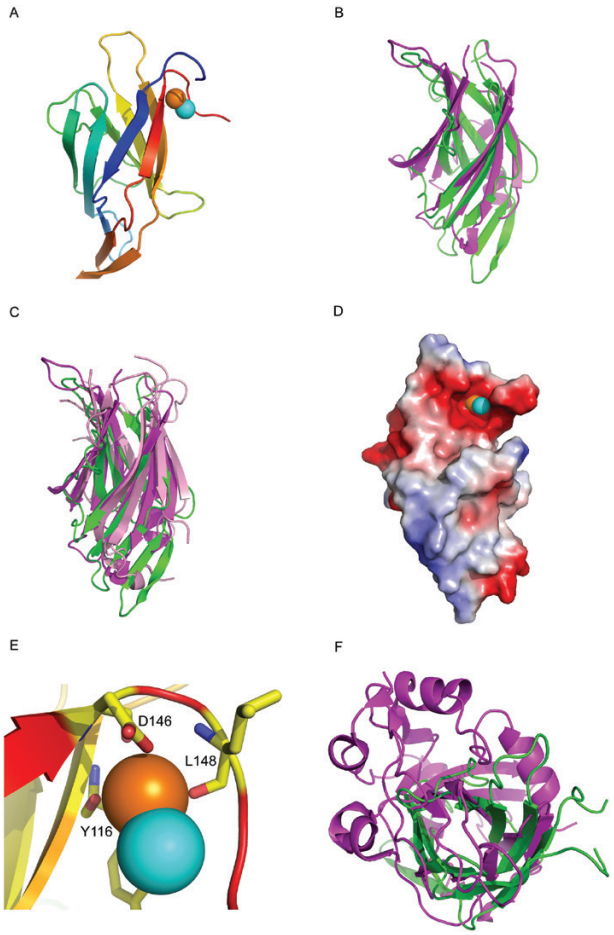

Fig. 1. Crystal structure of PevD1. (A) Overall structure of PevD1. The molecule is shown as a ribbon in rainbow color, blue at the N terminus and red at the C terminus. The coordinated calcium and chloride ions are shown as spheres of brown and cyan color, respectively. (B) Structural superimposition of PevD1 and the C2 domain of synaptotagmin IV (PDB code 1W16). Both structures are shown as a ribbon and colored with green for PevD1 and magenta for C2. (C) Structural superimposition of PevD1 and the C2 domain of phosphatidylinositol-4,5-bisphosphate 3-kinase (PDB code 3PS6). The structures are shown as in (B). (D) Surface charge potential of PevD1. Blue represents positive charge and red negative charge. Calcium and chloride ions are shown as in (A). (E) Details of calcium binding. The residues involved in calcium binding are labeled and shown as a stick model. The calcium and chloride ions are shown as in (A). (F) Structural superimposition of PevD1 and NLP. The structures are shown as a ribbon and top-viewed along the central axis of the β-barrel for clarity. PevD1 is colored in green and NLP in magenta.

repetitively (Supplementary Fig. S1). The bimolecular fluorescence complementation assays in tobacco leaf epidermal cells and *in vitro* GST pull-down assays further confirmed these interactions (Fig. 2 and Supplementary Fig. S1). Since the purified CRY2 from *E. coli* is known to be inactive (Worthington *et al.*, 2003), the pull-down assay for CRY2–NRP was performed with transgenic *GFP-CRY2* plants.

Since *V. dahliae* hyphae are known to penetrate root cells and PevD1 is a secreted protein, we postulated that PevD1 secreted by the fungus may enter the cytoplasm of root cells. To confirm this, immunostaining with anti-PevD1 antibodies was carried out in Arabidopsis roots infected with *V. dahliae*. Laser confocal scanning microscopy showed that PevD1 mainly localized to the plasma membrane, with

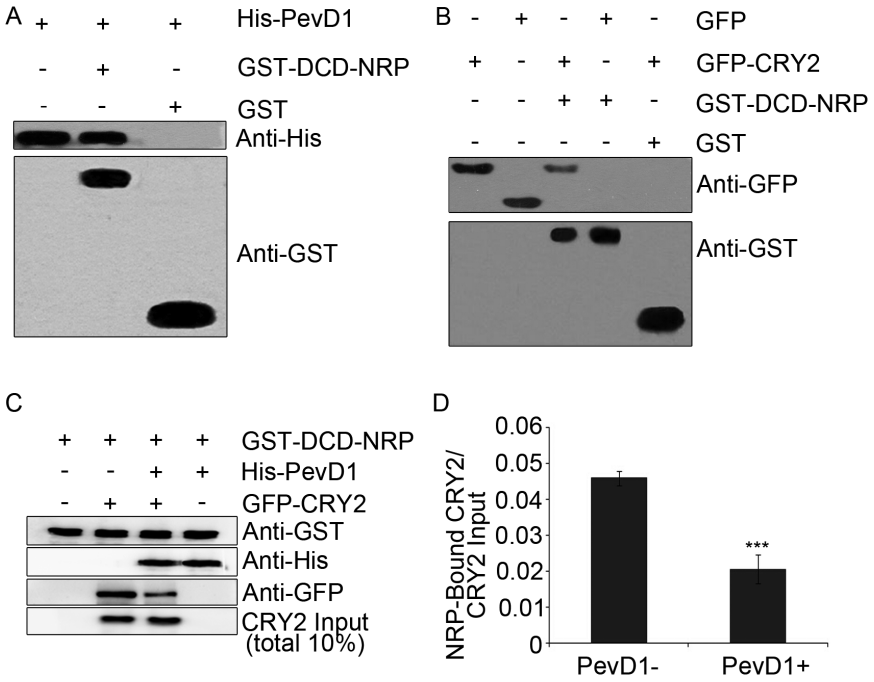

Fig. 2. Interactions of PevD1, NRP, and CRY2. (A) Interaction between PevD1 and NRP detected by GST pull-down. Upper panel shows detection by anti-6×His antibody, lower panel detection by anti-GST antibody. (B) Interaction between NRP and CRY2 detected by GST pull-down. Upper panel shows detection by anti-GFP antibody, lower panel detection by anti-GST antibody. (C) The disturbance of PevD1 in the interaction between NRP and CRY2 detected by GST pull-down. The three panels show detection by anti-GST antibody, anti-6×His antibody, and anti-GFP antibody, respectively. CRY2 input was used for control. (D) The binding ratio of CRY2 calculated in (C). Protein amounts were quantified by Image J from three repeat experiments. The amount of CRY2 input was set to 1. The statistically significant difference between without and with PevD1 was calculated with Student's *t*-test: ***P<0.001.

cytoplasmic puncta also observed (Supplementary Fig. S2A). The fluorescent lipophilic dye FM4-64 is widely used to trace endocytosis and to outline endosomes. After *V. dahliae* infection, partial colocalization of PevD1 and FM4-64 could be observed, indicating that PevD1 could be found on endosomes (Supplementary Fig. S3A–E). A fractionation assay further confirmed the presence of PevD1 in the cytoplasm (Supplementary Fig. S3F). *V. dahliae* penetrates the host through the roots but could spread through the xylem upwards to vascular tissues of leaves. Indeed, PevD1 was detected in Arabidopsis leaves 5 d after *V. dahliae* infection of the roots (Supplementary Fig. S2B).

CRY2–NRP and NRP–PevD1 interact bilaterally; thus we speculated that PevD1 might interfere with the interaction of CRY2–NRP to function as an inhibitor of this specific interaction. To address this, the GST pull-down assay was performed for NRP–CRY2 in the absence or presence of PevD1. As expected, the presence of PevD1 reduced the interaction of CRY2–NRP significantly (Fig. 2C, D).

NRP tethers CRY2 in the cytoplasm in a blue light-independent manner

Since CRY2 functions in the nucleus (Liu *et al.*, 2016) and NRP is predominantly localized in the cytoplasm (Hoepflinger *et al.*, 2011), we investigated whether NRP could affect CRY2 function by changing its subcellular localization. Firstly, *NRP-RFP* and *GFP-CRY2* were inoculated together into the leaves of *N. benthamiana* and their localization patterns were examined. *GFP-CRY2* was used for comparison. Indeed, when coexpressed with NRP–RFP, a significant portion of GFP–CRY2 signals were detected in the cytoplasm, where it colocalized with NRP. Since CRY2 functions are generally blue light dependent, we repeated the experiment in blue light. The cytoplasmic tethering of CRY2 by NRP was not dependent on blue light. Blue light treatment did have some minor effect on CRY2 distribution in *NRP-RFP GFP-CRY2* double transgenic plants, which might be due to degradation of nuclear CRY2 under blue light (Supplementary Fig. S4).

To confirm the NRP–CRY2 interaction *in vivo*, several transgenic plants were generated. *PevD1-RFP* transgenic and *NRP-RFP GFP-CRY2* double transgenic (OX) lines were generated, and *NRP-GFP* and *GFP-CRY2* transgenic lines, together with *nrp* and *cry2* null mutants (KO) were obtained (Hoepflinger *et al.*, 2011; Yu *et al.*, 2010). All lines were validated by RT-PCR. Purified PevD1–RFP protein triggered the hypersensitive response on *N. benthamiana* leaves as PevD1 did, suggesting that the tagged protein is functional (Supplementary Fig. S2C).

The nucleus to cytoplasm shift of CRY2 in the presence of NRP was further confirmed in the *NRP-RFP GFP-CRY2* double transgenic line (Fig. 3). The intensity of the NRP–RFP signal appeared to be relatively low (Fig. 3B). We postulated that NRP could have a high turnover rate *in vivo*, or the discrepancy between the signal intensity in tobacco and Arabidopsis could be due to the difference between the transient and the stable transgenic system.

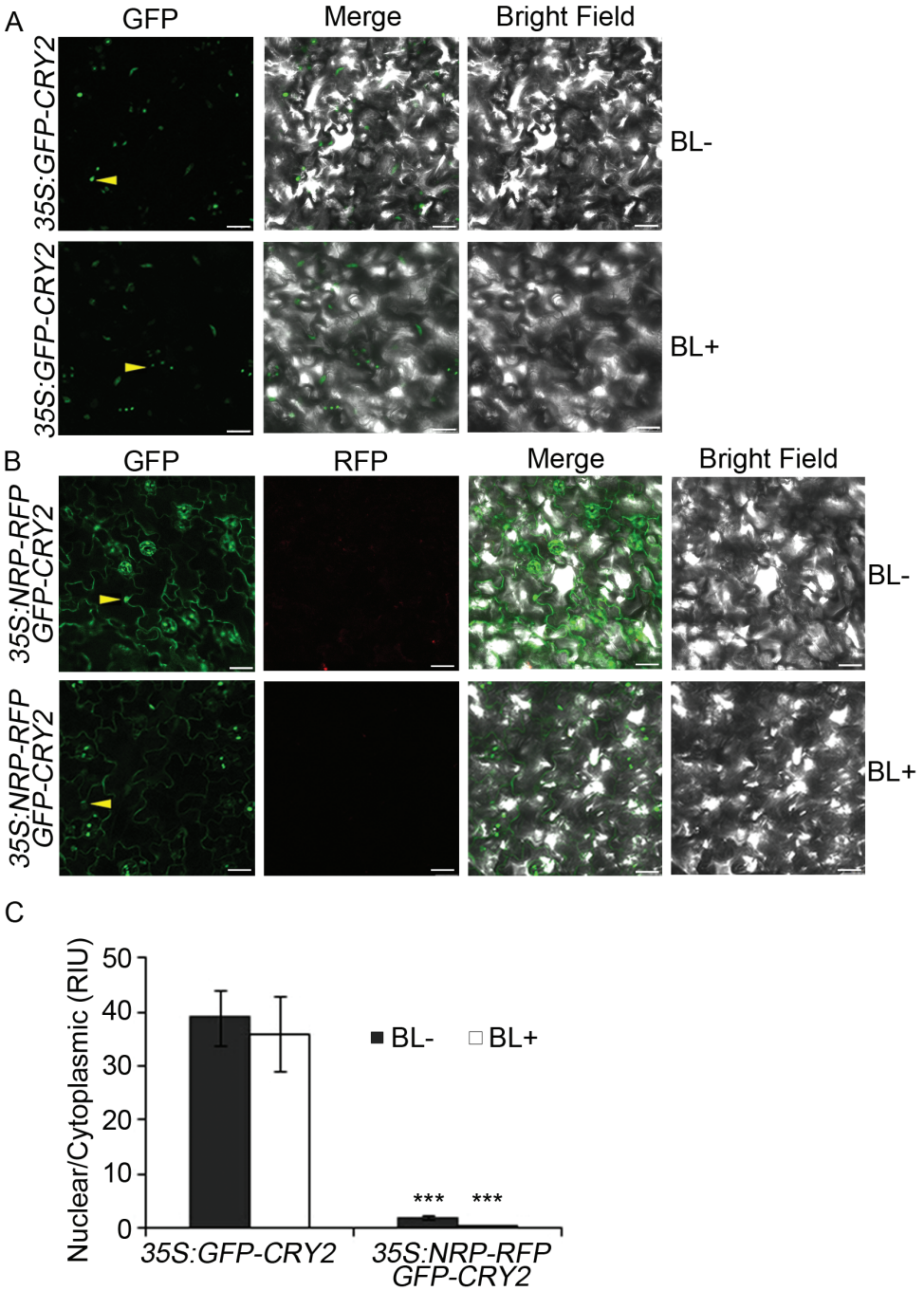

Fig. 3. The cytoplasm–nucleus distribution of CRY2 in Arabidopsis leaves. (A) Localization of GFP–CRY2 in Arabidopsis leaves under dark (BL–) and blue light (BL+). (B) Localization of NRP–RFP and GFP–CRY2 in Arabidopsis leaves under dark and blue light. (C) The nuclear–cytoplasmic distribution of GFP–CRY2 in (A) and (B) was quantified by ImageJ and calculated by the relative intensity unit (RIU) formula: (nuclear GFP fluorescence intensity)/(cytoplasmic GFP fluorescence intensity). More than 50 cells from five independent plants were used. Asterisks indicate significant differences of CRY2 distribution between absence and presence of NRP–RFP coexpression. The statistically significant differences were calculated with Student's *t*-test: ***$P<0.001$, $n\geq50$. Scale bar: 25 μm in (A) and (B). Bars in (C) show SD. Arrow heads indicate representative nuclei. (This figure is available in color at *JXB* online.)

Furthermore, coimmunoprecipitation experiments for NRP and CRY2 using *NRP-RFP GFP-CRY2* double transgenic plants showed that NRP and CRY2 could interact in a blue light-independent manner (Fig. 4A). We further compared the nuclear and the cytoplasmic distribution of CRY2 in *GFP-CRY2* plants with that of transgenic plants carrying both *NRP-RFP* and *GFP-CRY2* by subcellular fractionation assay. Proteins prepared from the rosette leaves of 4-week-old plants were fractionated into the cytoplasmic and nuclear fractions and CRY2 distribution was analysed. CRY2 was detected only in the nucleus in *GFP-CRY2* and in both cytoplasm and nucleus in *NRP-RFP GFP-CRY2* double transgenic plants (Fig. 4B, F). Fractionation experiments were also carried out under blue light for comparison. The results were the same as those obtained from the dark treatment (Fig. 4C, F), suggesting that the tethering of CRY2 in

the cytoplasm by NRP is blue light independent. So far, a reliable quantification of the nuclear–cytoplasmic partitioning of endogenous CRY2 in the wild-type, *PevD1-RFP*, and *NRP-GFP* transgenic plants could not be achieved, possibly due to the limited sensitivity of available anti-CRY2 antibodies.

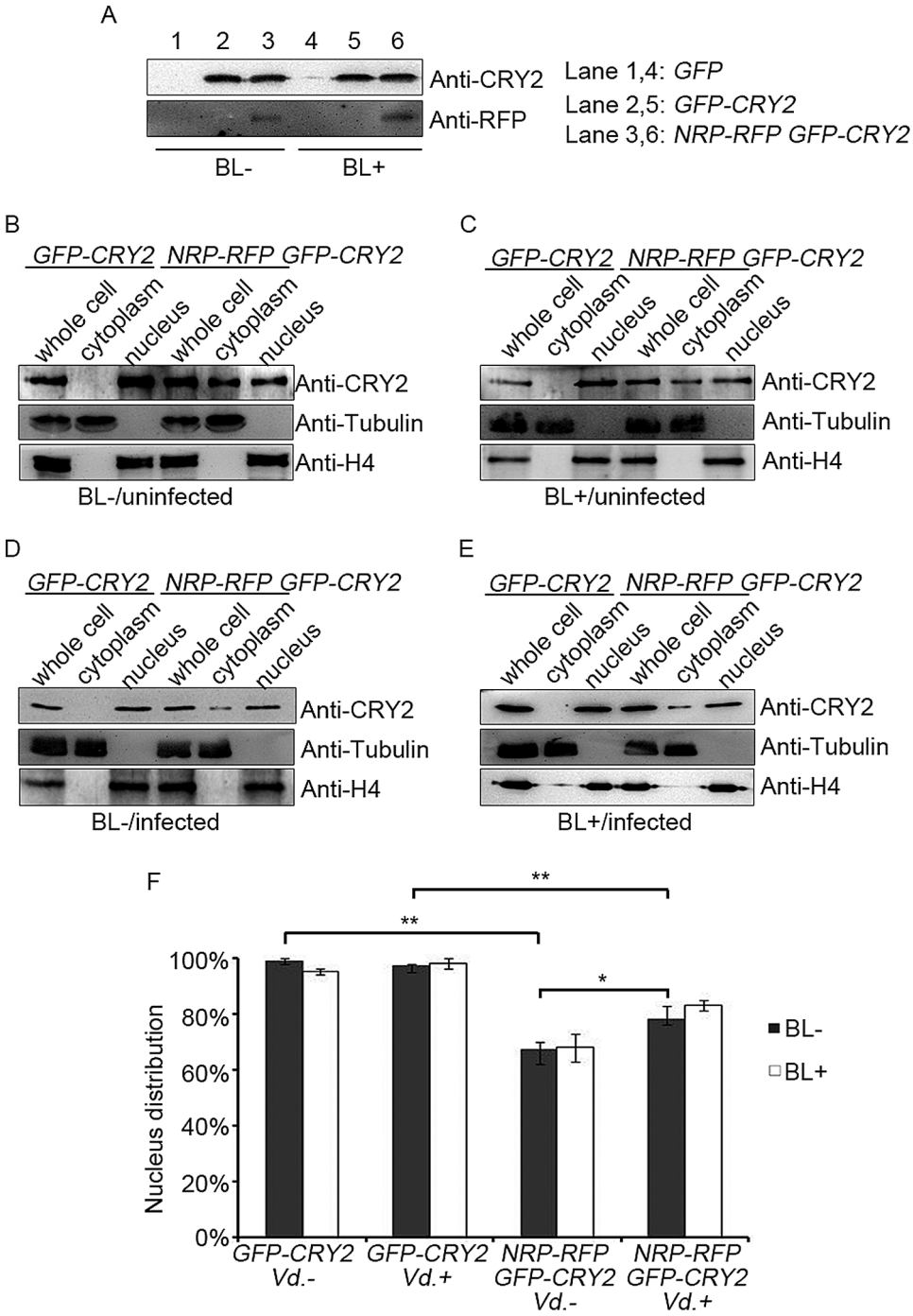

Fig. 4. Interaction between NRP and CRY2 in transgenic plants and the cytoplasm–nucleus distribution of CRY2 under *V. dahliae* infection and blue light. (A) The interaction between NRP and CRY2 was detected by GFP-Trap assay. Upper panel shows detection by anti-CRY2 antibody, and the lower panel detection by anti-RFP antibody. (B) The cytoplasm–nucleus distribution of uninfected *35S:GFP-CRY2* and *35S:NRP-RFP GFP-CRY2* transgenic plants under dark. (C) The cytoplasm–nucleus distribution of uninfected *35S:GFP-CRY2* and *35S:NRP-RFP GFP-CRY2* transgenic plants under blue light. (D) The cytoplasm–nucleus distribution of infected *35S:GFP-CRY2* and *35S:NRP-RFP GFP-CRY2* transgenic plants under dark. (E) The cytoplasm–nucleus distribution of infected *35S:GFP-CRY2* and *35S:NRP-RFP GFP-CRY2* transgenic plants under blue light. All the three panels in (B–E) show detection by anti-CRY2 antibody, anti-tubulin antibody, and anti-histone H4 antibody respectively. (F) The cytoplasm–nucleus distribution of CRY2 in transgenic plants in (B–E) was quantified by ImageJ. Three biological replicates were used for calculation. Asterisks indicate significant differences of CRY2 distribution between absence and presence of NRP–RFP coexpression, or between without and with *V. dahliae* infection. The comparisons were made for dark treatment only. The statistically significant differences were calculated with Student's *t*-test: **P*<0.05; ***P*<0.01. Bars in (F) show SD. *Vd*: *V. dahliae* infection; BL: blue light treatment.

The interaction between CRY2 and NRP is disturbed during V. dahliae *infection*

Since NRP could change the subcellular localization of CRY2, and PevD1 interacts with NRP, we speculated that CRY2 localization might be influenced by PevD1 indirectly during *V. dahliae* infection. To address this, the localization of CRY2 was determined in *V. dahliae*-infected plants. In *GFP-CRY2* plants, localization of CRY2 was not affected by fungal infection. In contrast, in *NRP-RFP GFP-CRY2* plants, the cytoplasmic distribution of CRY2 was reduced substantially upon infection, suggesting that NRP function might be antagonized by PevD1 during infection. These experiments were also repeated under blue light. Consistent with the observation above, blue light treatment had no visible effect on NRP–CRY2 interaction upon infection (Fig. 4D–F).

NRP rescues the dwarf phenotype of CRY2 overexpression

Our observations suggest that NRP changes CRY2 localization, which might lead to loss of function of CRY2. Since *GFP-CRY2* has a dwarf phenotype with shorter height and smaller rosette, *NRP-RFP* was ectopically expressed in *GFP-CRY2* and the phenotype was observed. In the double transgenic line, the dwarf phenotype of *GFP-CRY2* was almost completely rescued (Fig. 5). Therefore, NRP–CRY2 interaction may be required for plant development, and be modulated in the pathogenic response.

PevD1–NRP–CRY2 influences flowering time in Arabidopsis

To understand the physiological consequences of the interactions of PevD1 with NRP and NRP with CRY2, several genetic experiments were performed. Flowering-related phenotypes were documented and statistically evaluated for the OX and KO lines. *cry2* null mutant is late-flowering, which is consistent with a previous report (Guo *et al.*, 1998). Interestingly, *PevD1-RFP* plant bolted and flowered 3 d earlier than the wild-type, with statistical significance (P=0.001). In contrast, *NRP-GFP* was on average 4 d later than the wild-type both in bolting and flowering. Surprisingly, flowering time of *nrp* was not statistically different from that of the wild-type (Fig. 6A–D). Since there are six other DCD-containing proteins in Arabidopsis, this observation could be due to functional redundancy (Supplementary Fig. S5).

To explore the possible roles of PevD1–NRP–CRY2 interaction in flowering control upon *V. dahliae* infection, the lines used above were germinated on plates, inoculated with *V. dahliae* at day 7, and transplanted to soil on day 10. Compared with plants sown directly in soil (Fig. 6D), the plants generally flowered approximately 2 d earlier even without fungal infection (Fig. 6E). The infected wild-type flowered 4 d earlier than the untreated plants (Fig. 6E). The infection had little influence on the flowering time of *PevD1-RFP* and *NRP-GFP*, indicating a saturation effect by overexpression of these proteins on flowering. *nrp* and *GFP-CRY2* flowered approximately 2 d earlier upon *V. dahliae* infection than in the uninfected controls. The *cry2* mutant flowered much later than the wild-type with or without infection (12 and 14 d, respectively), validating the role of CRY2 as a master regulator of flowering (Fig. 6E). The flowering time of *cry2* was shortened by 6 d by infection, suggesting that other regulators of flowering may also respond to *V. dahliae*.

A PevD1 transgenic plant is also produced in the background of *cry2*. The *PevD1-RFP cry2* transgenic line is similar to the *cry2* mutant in flowering time, i.e. late flowering yet flowering earlier upon infection, suggesting that PevD1–NRP–CRY2 interaction could play a major role in flowering control, whereas other flowering pathways are likely involved following *V. dahliae* infection (Fig. 6E).

The mechanism of the PevD1–NRP–CRY2 pathway in flowering time control

It is well established that, by regulating the activation of flowering-time genes, such as *CIB*, *CO*, *FT*, and *SOC1*, CRY2 positively controls flowering time in Arabidopsis (Guo *et al.*, 1998; Liu *et al.*, 2016). qRT-PCR on these flowering genes was performed to link the observed flowering time phenotypes to the CRY2-mediated signaling cascade. Overall, timing and intensity of induction of key flowering genes in all transgenic lines and null mutants was consistent with the phenotypes observed. Except for the late-flowering *NRP-GFP* and *cry2*, a major peak for gene expression appeared at day 31 when flowering began, and a subordinate peak at day 29 was also observed in some lines, especially for FT in wild-type and *PevD1-RFP* (Supplementary Fig. S6). These data further supported the existence of a PevD1–NRP–CRY2 pathway that leads to early flowering in Arabidopsis.

Collectively, our study revealed that PevD1 functions as a fungal effector with a C2-domain-like structure, which interacts with the versatile stress-responsive protein NRP. We also showed that NRP can tether CRY2 in the cytoplasm and modulate the CRY2-dependent flowering pathway, a process that could be exploited by fungi during infection through effectors such as PevD1. A model is presented to outline these discoveries (Fig. 7).

Discussion

The C2-like structure of PevD1 may represent a common fold of fungal toxins

In this study, we first obtained the crystal structure of a *V. dahliae* effector protein, PevD1. Since most reported fungal effectors have not been successfully categorized, we wanted to see if a C2-like, membrane-targeting structure could represent a typical fold. Indeed, sequence analyses identified a large family of proteins that share low homology in their primary sequences, but have highly similar three-dimensional structures (Supplementary Fig. S2D). These proteins comprise ~150 amino acids and contain two pairs of highly conserved disulfide bonds. Among them is Alt a 1 from *Alternaria alternata*, which, besides being a plant pathogen, is also a major

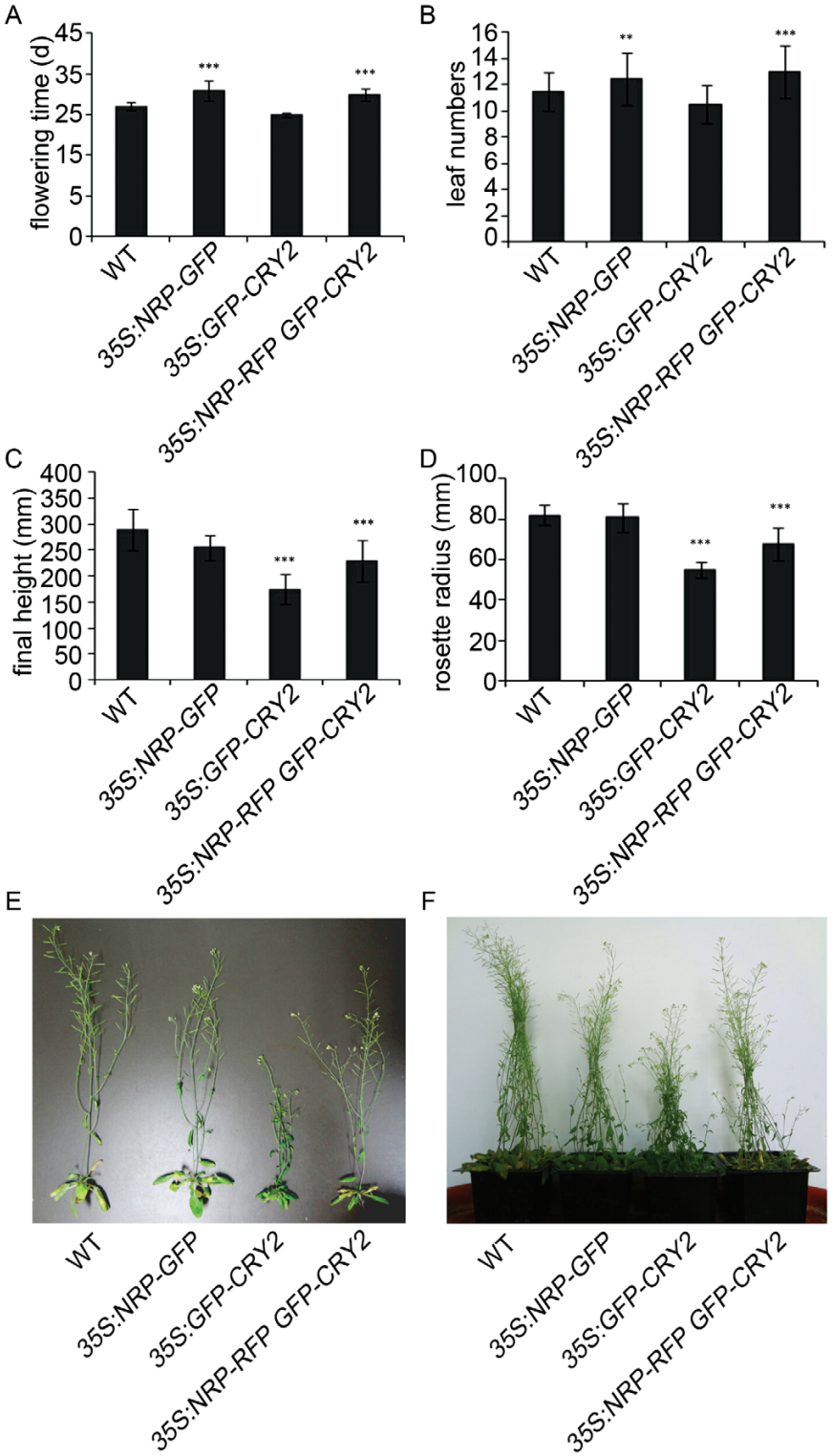

Fig. 5. The phenotypes of *NRP-RFP GFP-CRY2* double transgenic plants. Mean values and standard deviations are shown (n>20 for each line). (A) Flowering time of wild-type, *35S:NRP-GFP*, *35S:GFP-CRY2*, and *35S:NRP-RFP GFP-CRY2*. (B) Number of rosette leaves upon flowering in each line. (C) Final plant heights in each line. (D) Final rosette radius in each line. (E) Representative plants from (C) and (D). (F) Photo showing the final plant heights. The statistically significant differences between each line and WT were calculated with Student's t-test in (A–D): $^{**}P$<0.01; $^{***}P$<0.001. Bars in (A–D) show SD. (This figure is available in color at *JXB* online.)

human allergen (Salo *et al.*, 2005) (Supplementary Fig. S7). Furthermore, we have recently crystallized another family member, MoHrip1, from the major rice fungal pathogen *Magnaporthe oryzae*, and this protein indeed shares a similar fold with PevD1 despite their low sequence homology (Zhang *et al.*, 2013*a*). We speculate that like NLPs, PevD1-like proteins may function similarly in their respective hosts during infection.

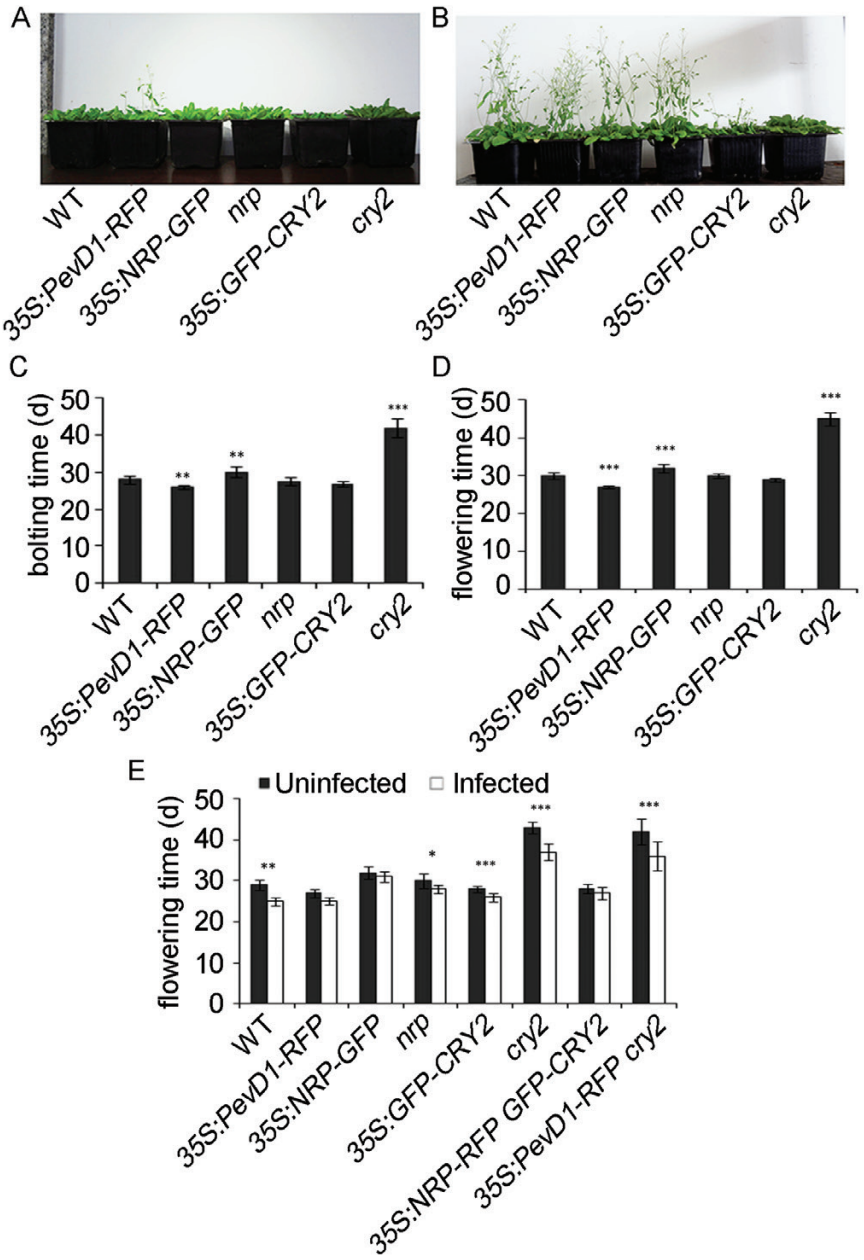

Fig. 6. Flowering time of wild-type, *35S:PevD1-RFP*, *35S:NRP-GFP*, *nrp*, *35S:GFP-CRY2*, *cry2*, *35S:NRP-RFP GFP-CRY2*, and *35S:PevD1-RFP cry2*. Mean values and standard deviations are shown (n>30 for each line). (A) *35S:PevD1-RFP* flowers earlier than other lines. Photo taken at day 29. (B) *Cry2* is late in flowering. Photo taken at day 36. (C) Bolting time of each line. (D) Flowering time of each line. (E) Flowering time before and after *V. dahliae* infection. Asterisks indicate significant differences between each line and WT for flowering time in (C) and (D). Asterisks indicate significant differences between uninfected and infected plants for flowering time in (E). The statistically significant differences were calculated with Student's t-test: *P<0.05; **P<0.01; ***P<0.001. Bars in (C–E) show SD. (This figure is available in color at *JXB* online.)

It is noteworthy that PevD1 has a C2 domain-like fold, with a calcium ion in the C-terminal acidic pocket (Fig. 1D). C2 has long been recognized as a unique lipid-binding domain, and many plant proteins with C2 domains are regulators of intracellular trafficking (Wang, 2000; Cho and Stahelin, 2005). Furthermore, essential trafficking and signaling proteins, such as phosphoinositide 3-kinase and phosphatase and tensin homologue (PTEN), have C2-like domains in their structures that facilitate their membrane docking and protein–protein interaction (Cain and Ridley, 2009; Mulgrew-Nesbitt *et al.*, 2006). It has been postulated that calcium can substitute for the magnesium ion identified in the NLP crystal structure in physiological environments to mediate docking of NLP to the target membrane (Ottmann *et al.*, 2009*b*). Thus, C2 and C2-like domains may be considered an important class of regulators in various trafficking/signaling routes, including fungal invasion of plant cells. NLP can induce pores in the plasma membrane to induce host cell damage (Qutob *et al.*, 2006; Küfner *et al.*, 2009; Ottmann *et al.*, 2009*a*), and can also induce plant immunity by acting as a microbe-associated molecular pattern (Oome *et al.*, 2014). Alt a 1 was shown to regulate the enzymatic activity of PR5 (Gómez-Casado *et al.*, 2014). PevD1 functions inside plant cells by interacting with NRP, but a plasma membrane

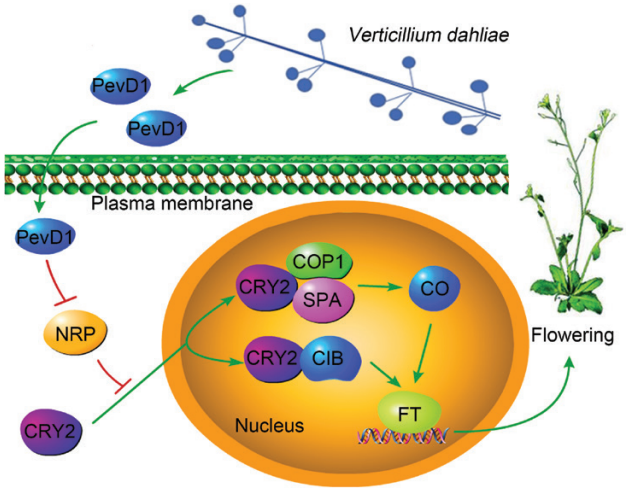

Fig. 7. The model proposed for this study. NRP interacts with PevD1 and regulates the subcellular localization of CRY2. (This figure is available in color at *JXB* online.)

localization and interaction cannot be precluded at this stage. As fungal effectors belonging to divergent subfamilies, these proteins might have similarities in folding but have evolved different pathogenic mechanisms.

CRY2 could be cytosolically localized under specific conditions

CRY2 is a protein that undergoes blue-light-dependent phosphorylation, ubiquitination, and degradation all in the nucleus (Guo *et al.*, 1999; Kleiner *et al.*, 1999; Yu *et al.*, 2007). Interestingly, the interaction between NRP and CRY2 is independent of blue light stimulation. Considering that all known modifications of CRY2 protein, such as phosphorylation and ubiquitination, only take place in the nucleus in a blue light-dependent way, the portion of CRY2 retained by NRP in the cytoplasm might be dysfunctional. Thus the tethering of CRY2 could happen after CRY2 protein is synthesized in the cytoplasm, and can be considered a way of reducing the amount of functional CRY2 under severe stress conditions. Our physiological and genetic analyses are consistent with this hypothesis. Otherwise, the cytoplasmic CRY2 might have yet unknown functions, as in the case of CRY1. Cytoplasmic CRY1 has been reported to promote primary root growth and cotyledon expansion in blue light, thus functioning in a way distinct from nuclear CRY1 (Wu and Spalding, 2007). Further analysis is required to elucidate the possible function of cytoplasmic CRY2.

Plants may modulate flowering time by the NRP–CRY2 pathway

How the timing of flowering is determined has been a focus of plant developmental and physiological studies, and a complex network has been constructed over time (Levy and Dean, 1998). Nonetheless, no specific pathway has been identified to illustrate how the flowering machinery is manipulated *in vivo* to respond to environmental stresses. In this study, we establish a link between a fungal elicitor, PevD1, and the key regulator of flowering time CRY2, and demonstrate that they are connected by the DCD domain-containing protein NRP. We show that, by tethering CRY2 in the cytoplasm, NRP could suppress CRY2 function in flowering time control. Interestingly, expression of NRP is down-regulated prior to bolting in wild-type Arabidopsis (Hoepflinger *et al.*, 2011). Additionally, other DCD domain-containing proteins, such as GDA1, have similar expression patterns as NRP (Li *et al.*, 1998). GDA1 transcript accumulates in pea during the vegetative phase but rapidly disappears after entering the reproductive phase. The transition is mediated by a change of the light period from short to long days. Therefore, the involvement of DCD domain-containing proteins in flowering time control may represent a general pathway for flowering plants—when environmentally challenged, these proteins may interact with CRY2 or other key players to modulate flowering time. It has been known that AtNRP is a stress responsive protein (Hoepflinger *et al.*, 2011), and GmNRPs participate in endoplasmic reticulum and osmotic stress signaling (Costa *et al.*, 2008). By modulating the expression of stress-responsive NRP, plants may obtain a versatile regulation of flowering time controlled by CRY2, leading to better survival in unfavorable environments.

Fungi may target NRPs for efficient infection by PevD1-like effectors

V. dahliae is a soil-borne pathogen. The fungal mycelia enter the plant root and reach the vessels of the root vasculature, where the spores are produced and carried upward through the transpiration stream (Zhao *et al.*, 2014). By utilization of secreted toxins like PevD1, the fungus may gain opportunities to spread along the xylem by regulating the defense response through interaction with NRP. Unlike another well-known effector from *V. dahliae*, Ave1, which functions through its plasma membrane-localized receptor Ve1 (de Jonge *et al.*, 2012; Liebrand *et al.*, 2013), PevD1 might enter the host cells and function by interacting with cytosolic NRP (Supplementary Figs S2 and S3). Immunolocalization of PevD1 showed that it mainly localizes to the plasma membrane but is also present in the cytoplasm (Supplementary Fig. S2A). When expressed in plant cells, either stable or transient, PevD1 also localizes in the cytoplasm or at the plasma membrane. Fungal effectors functioning through both plasma membrane-localized receptors and cytoplasm-localized receptors have been identified, especially in rice blast fungus *M. oryzae* (Martin-Urdiroz *et al.*, 2016; Yan and Talbot, 2016). In our study, PevD1 is found to interact with cytosolic NRP, yet a potential membrane-localized receptor for PevD1 cannot be precluded. Two functionally studied effectors from *V. dahliae*, Ave1 and VdIsc1, play their roles *in planta* extracellularly and intracellularly, respectively (de Jonge *et al.*, 2012; Liu *et al.*, 2014). Sequence analyses identified a large family of proteins that share similarity with PevD1 from various fungi (Supplementary Fig. S2D) (Salo *et al.*, 2005). We speculated that these PevD1-like fungal proteins might exert their function on respective hosts by a conserved mechanism.

Our study shows that *cry2* flowers earlier upon *V. dahliae* infection than when not infected (Fig. 6E), indicating flowering regulators besides CRY2, such as the gibberellin pathway, might be affected in *V. dahliae* infection. Since *V. dahliae* secretes hundreds of effectors during infection, effectors other than PevD1, or interacting partners other than NRP, are likely involved in the modulation of flowering. It has been shown that during the infection of *P. syringae* and *H. arabidopsidis*, mis-expression of clock genes such as circadian clock-associated 1 (*CCA1*) and late and elongated hypocotyl (*LHY*) compromises basal and *R*-gene-mediated resistance (Zhang *et al.*, 2013*b*). More crosstalk between flowering and plant immunity is expected to be uncovered in future.

NRP is promptly induced by various stresses and is known to contribute to plant adaption in unfavorable environments (Costa *et al.*, 2008; Hoepflinger *et al.*, 2011). By antagonizing NRP with PevD1, *V. dahliae* might acquire two advantages: firstly, the early flowering induced by PevD1 might aid the spread of spores to above-ground organs (stem and leaves). Secondly, the local HR response elicited by NRP might be antagonized and thus favor the spread of *V. dahliae*. Whether *PevD1*-null *V. dahliae* is more or less virulent on Arabidopsis awaits future investigation.

The dwarf and early-flowering phenotypes of *GFP-CRY2* are highly similar to the phenotypes of *V. dahliae*-infected Arabidopsis (Veronese *et al.*, 2003), and we noticed that overexpression of NRP in *GFP-CRY2* can almost completely restore these phenotypes (Fig. 5). In our working model, NRP could serve as a molecular switch between vegetative growth and floral transition upon fungal invasion. Under normal growth conditions, NRP negatively regulates CRY2-mediated flowering. Upon severe *V. dahliae* infection, the PevD1–NRP interaction could activate the CRY2-mediated flowering pathway, leading to early flowering of the plant.

In summary, our results identify a new pathway that is exploited by *V. dahliae* to modulate the transition between vegetative growth and flowering in the host plant, and provide an answer to why the infection of *V. dahliae* in plants such as cotton and Arabidopsis can induce early flowering. New mechanisms could be uncovered about how plants evolved to modulate their developmental programs to better survive diverse stresses and proliferate, and how fungi modulate their infection strategies through versatile fungal effectors.

Supplementary data

Supplementary data are available at *JXB* online.

Fig. S1. Interactions of PevD1 with NRP, and NRP with CRY2.

Fig. S2. The characterization of PevD1.

Fig. S3. PevD1 secreted by *V. dahliae* could translocate into Arabidopsis root cells.

Fig. S4. NRP and CRY2 colocalization and cytoplasm-nucleus distribution in *N. benthamiana* leaves.

Fig. S5. Sequence alignment of DCD-containing proteins in Arabidopsis.

Fig. S6. Quantitative RT-PCR of CO, FT, FLC, CRY2, and SOC1.

Fig. S7. Superimposition of PevD1 and Alt a 1.

Table S1. X-ray crystallographic data and refinement statistics for PevD1.

Table S2. Primer sequences used in this study.

Data deposition

Atomic coordinates and structural factors of PevD1 have been deposited in the RCSB Protein Data Bank under ID code 5XMZ.

Funding

XL is supported by the National Natural Science Foundation of China (31370925 and 31640024). QG is supported by the National Natural Science Foundation of China (31401179 and 31671419).

Acknowledgements

We thank Drs Yongfu Fu, Hongtao Liu, Jiafu Long, and Raimund Tenhaken for providing constructs, mutants, and transgenic lines. We also thank Dr Hans Bohnert for critical reading of the manuscript.

Author contributions

XL and QG conceived the project and designed the experiments. DQ contributed essential materials. RZ, TZ, LH, ML, MX, YL, and DH performed the experiments. XL and QG analysed the data. XL and QG wrote the paper. The authors declare that they have no conflict of interest.

References

Cain RJ, Ridley AJ. 2009. Phosphoinositide 3-kinases in cell migration. Biology of the Cell **101,** 13–29.

Campbell RE. 1989. Biological control of microbial plant pathogens. Cambridge: Cambridge University Press.

Cho W, Stahelin RV. 2005. Membrane-protein interactions in cell signaling and membrane trafficking. Annual Review of Biophysics and Biomolecular Structure **34,** 119–151.

Corbalan-Garcia S, Gómez-Fernández JC. 2014. Signaling through C2 domains: more than one lipid target. Biochimica et Biophysica Acta **1838,** 1536–1547.

Costa MD, Reis PA, Valente MA, Irsigler AS, Carvalho CM, Loureiro ME, Aragão FJ, Boston RS, Fietto LG, Fontes EP. 2008. A new branch of endoplasmic reticulum stress signaling and the osmotic signal converge on plant-specific asparagine-rich proteins to promote cell death. The Journal of Biological Chemistry **283,** 20209–20219.

de Jonge R, van Esse HP, Maruthachalam K, *et al.* 2012. Tomato immune receptor Ve1 recognizes effector of multiple fungal pathogens uncovered by genome and RNA sequencing. Proceedings of the National Academy of Sciences, USA **109,** 5110–5115.

Friml J, Benková E, Mayer U, Palme K, Muster G. 2003. Automated whole mount localisation techniques for plant seedlings. The Plant Journal **34,** 115–124.

Genoud T, Buchala AJ, Chua NH, Métraux JP. 2002. Phytochrome signalling modulates the SA-perceptive pathway in Arabidopsis. The Plant Journal **31,** 87–95.

Gómez-Casado C, Murua-García A, Garrido-Arandia M, González-Melendi P, Sánchez-Monge R, Barber D, Pacios LF, Díaz-Perales

A. 2014. Alt a 1 from *Alternaria* interacts with PR5 thaumatin-like proteins. FEBS Letters **588,** 1501–1508.

Griebel T, Zeier J. 2008. Light regulation and daytime dependency of inducible plant defenses in Arabidopsis: phytochrome signaling controls systemic acquired resistance rather than local defense. Plant Physiology **147,** 790–801.

Guo H, Duong H, Ma N, Lin C. 1999. The Arabidopsis blue light receptor cryptochrome 2 is a nuclear protein regulated by a blue light-dependent post-transcriptional mechanism. The Plant Journal **19,** 279–287.

Guo H, Yang H, Mockler TC, Lin C. 1998. Regulation of flowering time by *Arabidopsis* photoreceptors. Science **279,** 1360–1363.

Han L, Liu Z, Liu X, Qiu D. 2012. Purification, crystallization and preliminary X-ray diffraction analysis of the effector protein PevD1 from *Verticillium dahliae*. Acta Crystallographica. Section F, Structural Biology and Crystallization Communications **68,** 802–805.

Hirayama T, Shinozaki K. 2010. Research on plant abiotic stress responses in the post-genome era: past, present and future. The Plant Journal **61,** 1041–1052.

Hoepflinger MC, Pieslinger AM, Tenhaken R. 2011. Investigations on N-rich protein (NRP) of *Arabidopsis thaliana* under different stress conditions. Plant Physiology and Biochemistry **49,** 293–302.

Jeong RD, Chandra-Shekara AC, Barman SR, Navarre D, Klessig DF, Kachroo A, Kachroo P. 2010. Cryptochrome 2 and phototropin 2 regulate resistance protein-mediated viral defense by negatively regulating an E3 ubiquitin ligase. Proceedings of the National Academy of Sciences, USA **107,** 13538–13543.

Kachroo A, Robin GP. 2013. Systemic signaling during plant defense. Current Opinion in Plant Biology **16,** 527–533.

Kissoudis C, van de Wiel C, Visser RG, van der Linden G. 2014. Enhancing crop resilience to combined abiotic and biotic stress through the dissection of physiological and molecular crosstalk. Frontiers in Plant Science **5,** 207.

Kleiner O, Kircher S, Harter K, Batschauer A. 1999. Nuclear localization of the Arabidopsis blue light receptor cryptochrome 2. The Plant Journal **19,** 289–296.

Küfner I, Ottmann C, Oecking C, Nürnberger T. 2009. Cytolytic toxins as triggers of plant immune response. Plant Signaling & Behavior **4,** 977–979.

Levy YY, Dean C. 1998. The transition to flowering. The Plant Cell **10,** 1973–1990.

Li HY, Guo ZF, Zhu YX. 1998. Molecular cloning and analysis of a pea cDNA that is expressed in darkness and very rapidly induced by gibberellic acid. Molecular & General Genetics **259,** 393–397.

Liebrand TW, van den Berg GC, Zhang Z, *et al*. 2013. Receptor-like kinase SOBIR1/EVR interacts with receptor-like proteins in plant immunity against fungal infection. Proceedings of the National Academy of Sciences, USA **110,** 10010–10015.

Liu B, Yang Z, Gomez A, Liu B, Lin C, Oka Y. 2016. Signaling mechanisms of plant cryptochromes in *Arabidopsis thaliana*. Journal of Plant Research **129,** 137–148.

Liu H, Yu X, Li K, Klejnot J, Yang H, Lisiero D, Lin C. 2008. Photoexcited CRY2 interacts with CIB1 to regulate transcription and floral initiation in *Arabidopsis*. Science **322,** 1535–1539.

Liu T, Song T, Zhang X, *et al*. 2014. Unconventionally secreted effectors of two filamentous pathogens target plant salicylate biosynthesis. Nature Communications **5,** 4686.

Liu Y, Li X, Li K, Liu H, Lin C. 2013. Multiple bHLH proteins form heterodimers to mediate CRY2-dependent regulation of flowering-time in *Arabidopsis*. PLoS Genetics **9,** e1003861.

Ludwig A, Tenhaken R. 2001. Suppression of the ribosomal L2 gene reveals a novel mechanism for stress adaptation in soybean. Planta **212,** 792–798.

Martin-Urdiroz M, Oses-Ruiz M, Ryder LS, Talbot NJ. 2016. Investigating the biology of plant infection by the rice blast fungus *Magnaporthe oryzae*. Fungal Genetics and Biology **90,** 61–68.

Miao W, Wang X, Li M, Song C, Wang Y, Hu D, Wang J. 2010. Genetic transformation of cotton with a harpin-encoding gene hpaXoo confers an enhanced defense response against different pathogens through a priming mechanism. BMC Plant Biology **10,** 67.

Mulgrew-Nesbitt A, Diraviyam K, Wang J, Singh S, Murray P, Li Z, Rogers L, Mirkovic N, Murray D. 2006. The role of electrostatics in protein-membrane interactions. Biochimica et Biophysica Acta **1761,** 812–826.

Oome S, Raaymakers TM, Cabral A, Samwel S, Bohm H, Albert I, Nurnberger T, Van den Ackerveken G. 2014. Nep1-like proteins from three kingdoms of life act as a microbe-associated molecular pattern in *Arabidopsis*. Proceedings of the National Academy of Sciences, USA **111,** 16955–16960.

Ottmann C, Luberacki B, Kufner I, *et al*. 2009*a*. A common toxin fold mediates microbial attack and plant defense. Proceedings of the National Academy of Sciences, USA **106,** 10359–10364.

Ottmann C, Rose R, Huttenlocher F, Cedzich A, Hauske P, Kaiser M, Huber R, Schaller A. 2009*b*. Structural basis for Ca^{2+}-independence and activation by homodimerization of tomato subtilase 3. Proceedings of the National Academy of Sciences, USA **106,** 17223–17228.

Pfaffl MW. 2001. A new mathematical model for relative quantification in real-time RT-PCR. Nucleic Acids Research **29,** e45.

Qutob D, Kemmerling B, Brunner F, *et al*. 2006. Phytotoxicity and innate immune responses induced by Nep1-like proteins. The Plant Cell **18,** 3721–3744.

Reis PA, Carpinetti PA, Freitas PP, *et al*. 2016. Functional and regulatory conservation of the soybean ER stress-induced DCD/NRP-mediated cell death signaling in plants. BMC Plant Biology **16,** 156.

Roden LC, Ingle RA. 2009. Lights, rhythms, infection: the role of light and the circadian clock in determining the outcome of plant-pathogen interactions. The Plant Cell **21,** 2546–2552.

Salo PM, Yin M, Arbes SJ Jr, Cohn RD, Sever M, Muilenberg M, Burge HA, London SJ, Zeldin DC. 2005. Dustborne *Alternaria alternata* antigens in US homes: results from the National Survey of Lead and Allergens in Housing. The Journal of Allergy and Clinical Immunology **116,** 623–629.

Schütze K, Harter K, Chaban C. 2009. Bimolecular fluorescence complementation (BiFC) to study protein-protein interactions in living plant cells. Methods in Molecular Biology **479,** 189–202.

Spoel SH, Dong X. 2008. Making sense of hormone crosstalk during plant immune responses. Cell Host & Microbe **3,** 348–351.

St Leger RJ, Joshi L, Roberts DW. 1997. Adaptation of proteases and carbohydrates of saprophytic, phytopathogenic and entomopathogenic fungi to the requirements of their ecological niches. Microbiology **143,** 1983–1992.

Tenhaken R, Doerks T, Bork P. 2005. DCD—a novel plant specific domain in proteins involved in development and programmed cell death. BMC Bioinformatics **6,** 169.

Veronese P, Narasimhan ML, Stevenson RA, Zhu JK, Weller SC, Subbarao KV, Bressan RA. 2003. Identification of a locus controlling *Verticillium* disease symptom response in *Arabidopsis thaliana*. The Plant Journal **35,** 574–587.

Wang B, Yang X, Zeng H, Liu H, Zhou T, Tan B, Yuan J, Guo L, Qiu D. 2012. The purification and characterization of a novel hypersensitive-like response-inducing elicitor from *Verticillium dahliae* that induces resistance responses in tobacco. Applied Microbiology and Biotechnology **93,** 191–201.

Wang W, Barnaby JY, Tada Y, Li H, Tör M, Caldelari D, Lee DU, Fu XD, Dong X. 2011. Timing of plant immune responses by a central circadian regulator. Nature **470,** 110–114.

Wang W, Vignani R, Scali M, Cresti M. 2006. A universal and rapid protocol for protein extraction from recalcitrant plant tissues for proteomic analysis. Electrophoresis **27,** 2782–2786.

Wang X. 2000. Multiple forms of phospholipase D in plants: the gene family, catalytic and regulatory properties, and cellular functions. Progress in Lipid Research **39,** 109–149.

Wei W, Davis RE, Nuss DL, Zhao Y. 2013. Phytoplasmal infection derails genetically preprogrammed meristem fate and alters plant architecture. Proceedings of the National Academy of Sciences, USA **110,** 19149–19154.

Worthington EN, Kavakli IH, Berrocal-Tito G, Bondo BE, Sancar A. 2003. Purification and characterization of three members of the photolyase/cryptochrome family blue-light photoreceptors from *Vibrio cholerae*. The Journal of Biological Chemistry **278,** 39143–39154.

Wu G, and Spalding EP. 2007. Separate functions for nuclear and cytoplasmic cryptochrome 1 during photomorphogenesis of Arabidopsis seedlings. Proceedings of the National Academy of Sciences, USA **104,** 18813–18818.

Wu L, Yang HQ. 2010. CRYPTOCHROME 1 is implicated in promoting R protein-mediated plant resistance to *Pseudomonas syringae* in *Arabidopsis*. Molecular Plant **3,** 539–548.

Yan X, Talbot NJ. 2016. Investigating the cell biology of plant infection by the rice blast fungus *Magnaporthe oryzae*. Current Opinion in Microbiology **34,** 147–153.

Yoo SK, Chung KS, Kim J, Lee JH, Hong SM, Yoo SJ, Yoo SY, Lee JS, Ahn JH. 2005. *CONSTANS* activates *SUPPRESSOR OF OVEREXPRESSION OF CONSTANS 1* through *FLOWERING LOCUS T* to promote flowering in Arabidopsis. Plant Physiology **139,** 770–778.

Yu X, Klejnot J, Zhao X, Shalitin D, Maymon M, Yang H, Lee J, Liu X, Lopez J, Lin C. 2007. Arabidopsis cryptochrome 2 completes its posttranslational life cycle in the nucleus. The Plant Cell **19,** 3146–3156.

Yu X, Liu H, Klejnot J, Lin C. 2010. The cryptochrome blue light receptors. The Arabidopsis Book **8,** e0135.

Zhang C, Liu X, Qiu D, Zeng H. 2013*a*. Purification, crystallization and preliminary X-ray diffraction analysis of the effector protein MoHrip1 from *Magnaporthe oryzae*. Acta Crystallographica. Section F, Structural Biology and Crystallization Communications **69,** 460–462.

Zhang C, Xie Q, Anderson RG, *et al*. 2013*b*. Crosstalk between the circadian clock and innate immunity in Arabidopsis. PLoS Pathogens **9,** e1003370.

Zhang X, Henriques R, Lin SS, Niu QW, Chua NH. 2006. *Agrobacterium*-mediated transformation of *Arabidopsis thaliana* using the floral dip method. Nature Protocols **1,** 641–646.

Zhao P, Zhao YL, Jin Y, Zhang T, Guo HS. 2014. Colonization process of *Arabidopsis thaliana* roots by a green fluorescent protein-tagged isolate of *Verticillium dahliae*. Protein & Cell **5,** 94–98.

Zuo Z, Liu H, Liu B, Liu X, Lin C. 2011. Blue light-dependent interaction of CRY2 with SPA1 regulates COP1 activity and floral initiation in Arabidopsis. Current Biology **21,** 841–847.

Zuo ZC, Meng YY, Yu XH, Zhang ZL, Feng DS, Sun SF, Liu B, Lin CT. 2012. A study of the blue-light-dependent phosphorylation, degradation, and photobody formation of *Arabidopsis* CRY2. Molecular Plant **5,** 726–733.